

# Ionization Dynamics of the Benzene–HF Complex: A Direct *ab Initio* Dynamics Study

Hiroto Tachikawa\*

Division of Molecular Chemistry, Graduate School of Engineering, Hokkaido University,  
Sapporo 060-8628, Japan

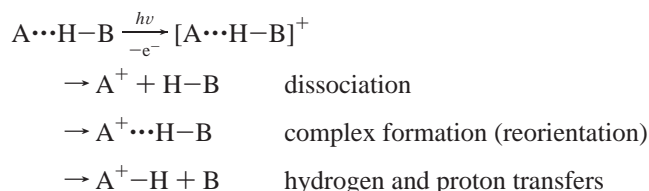
Received: May 17, 1999; In Final Form: June 18, 1999

Direct *ab initio* dynamics calculations have been carried out for the ionization processes of the benzene–HF (Bz–HF) complex in order to elucidate its mechanism and dominant factor on the reaction channels. The full dimensional potential energy surface (PES) including all degrees of freedom and its gradient were calculated at each time step in the dynamics calculation. The dynamics calculations of the neutral complex were carried out at constant temperatures 10 and 50 K in order to obtain the relevant structures at finite temperatures. It was found that the angle between a dipole moment of HF and the benzene  $C_6$  axis ( $\theta$ ) fluctuates largely due to the thermal energy. The Bz–HF complex has a nonrigid structure and a wide Franck–Condon region for the ionization. Using the geometrical configurations selected randomly from the neutral structures of Bz–HF, the trajectories for Bz<sup>+</sup>–HF system following the vertical ionization were calculated. Two reaction channels were obtained as products: one is the complex formation channel in which the complex composed of Bz<sup>+</sup>–FH is formed, while the other one is dissociation channel in which the trajectory directly leads to the dissociation product Bz<sup>+</sup> + HF. In the latter channel, the rotational quantum number of the dissociating HF molecule is calculated to be  $J = 1–3$ . The ionization from  $C_{6v}$  structure of neutral Bz–HF complex, calculated for comparison directly leads to the dissociation products Bz<sup>+</sup> + HF without the rotational excitation of the HF molecule. The calculations indicated that the ionization from the geometrical configuration with a large angle  $\theta$  leads to the complex formation Bz<sup>+</sup>–FH, whereas the trajectory with a small angle  $\theta$  leads to the dissociation products (Bz<sup>+</sup> + HF). The present calculations indicated that the angle  $\theta$  dominants strongly the preference of the reaction channels in the photoionization of Bz–HF complex. The mechanism was discussed on the basis of the theoretical results.

## 1. Introduction

In general, the collision in bi-molecular reaction ( $A + H–B$ ) takes place from the random collision angles. The reaction dynamics is therefore composed of the products from all collision angles. On the other hand, photoinitiated reaction from the corresponding complex ( $A\cdots H–B$ ) occurs only at specific angles which is governed by the geometrical configuration of the complex. The reaction of the complex would give the dynamics in which the collision angle is arranged. Therefore, the dynamics of the clusters and weakly bound complexes have been a topic of current interest.<sup>1–3</sup>

Several reaction channels, which are schematically expressed by the following reaction scheme, are concerned with the photoionization of the weakly bound complexes.



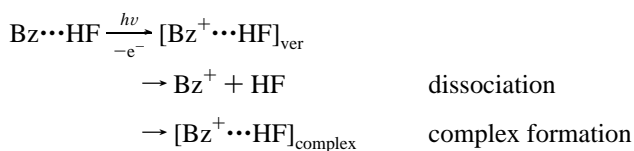
where A and B are heavy molecules, while H is hydrogen. The first channel is a direct dissociation of HB molecule from the parent cation A<sup>+</sup> ionized by photoirradiation. The second channel is a complex formation following the ionization. The structural change may be observed. The third channel is hydrogen and proton-transfer processes in (A<sup>+</sup> + H–B) or

(A + H<sup>+</sup>–B) systems, respectively. It is known that the former two channels are competing with each other in the case of low-ionization energy and in small clusters. However, its dominant factor on the preference of reaction channels is not clearly understood.

The photoionization of weakly bound cluster and complex plays an important role in gaseous ion chemistry and in interstellar cloud.<sup>1–3</sup> A large number of clusters have been investigated from both experimental and theoretical points of view. Benzene (Bz) is one of the prototype molecules which form  $\pi$ -type hydrogen bonded complexes with several proton-donor molecules such as HF,<sup>4</sup> HCl,<sup>5</sup> NH<sub>3</sub>,<sup>6</sup> and H<sub>2</sub>O.<sup>7</sup> Recently, the ionization processes of complexes have been investigated by several groups. Courty et al. investigated the ionization process of size-selected benzene–water clusters Bz(H<sub>2</sub>O)<sub>n</sub> by means of resonance-enhanced multiphoton ionization technique.<sup>8</sup> They showed that a proton transfer from the benzene cation to water cluster occurred by a ion–molecule reaction in the case of medium-sized clusters ( $n = 22–28$ ). Zwier and co-workers measured resonant two-photon ionization (R2PI) time-of-flight mass spectra of Bz(H<sub>2</sub>O)<sub>n</sub> complex ( $n = 1$  and 2). They found that the BzH<sub>2</sub>O<sup>+</sup> complex is formed by the photoionization of the Bz(H<sub>2</sub>O)<sub>n</sub> complex.<sup>3</sup> Recently, we applied direct *ab initio* dynamics method to the ionization processes of the Bz(H<sub>2</sub>O)<sub>n</sub> complex ( $n = 1$  and 2).<sup>11a</sup> It was found that two reaction channels, direct dissociation and complex formation channels, are concerned with the photoionization of the Bz(H<sub>2</sub>O)<sub>n</sub> complex.

The benzene–HF complex (Bz–HF) is also one of typical weakly bound complexes with a hydrogen bond between molecules.<sup>4,10</sup> The structure of the complex Bz–HF was measured by molecular beam experiment of Klemperer and co-workers.<sup>9</sup> Their experiment indicated that the hydrogen end of HF molecule points toward the benzene in the symmetric averaged structure. The hydrogen atom is  $\sim 2.25$  Å above the plane of Bz. The large amplitude motions present in this complex make it difficult to determine an equilibrium structure. Ab initio MO calculation of Bz–HF complex was carried out by Cheney et al.<sup>10</sup> Their HF/3-21G\* calculations indicated that the complex has  $C_s$  symmetry with a carbon–F atom distance of 3.42 Å, producing a largely distorted structure. However, the energy difference between the  $C_s$  and  $C_{6v}$  structures was negligibly small, suggesting that HF molecule can move easily on the benzene ring. These experimental and theoretical features imply that the Bz–HF complex has a wide Franck–Condon (FC) region for its ionization. However, the dynamics of ionization of Bz–HF is scarcely known.

In the present study, direct ab initio dynamics calculations<sup>11</sup> are carried out for the ionization processes of the Bz–HF complex which is very analogous to the Bz–H<sub>2</sub>O complex.<sup>11a</sup> From the energetics, it can be considered that two reaction channels



would proceed competitively in the Bz–HF system, where  $[\text{Bz}^+\cdots\text{HF}]_{\text{ver}}$  is a vertical ionized state formed by the ionization of neutral complex, and  $[\text{Bz}^+\cdots\text{HF}]_{\text{complex}}$  is a cation complex which is more stable in energy than the dissociation limit ( $\text{Bz}^+ + \text{HF}$ ). We focus our attention mainly on preference of the reaction channels after the photoionization of Bz $\cdots$ HF. The main purposes of this study are (1) to elucidate qualitatively the ionization dynamics of Bz–HF and (2) to determine origin of the preference of the reaction channels using the direct ab initio dynamics calculations.

## 2. Computational Methods

The classical trajectory calculations have been made on an analytically fitted potential energy surface as we have done previously.<sup>12</sup> However, it is not appropriate to predetermine the reaction surfaces of the present systems due to the large number of degrees of freedom ( $3N-6 = 36$  where  $N$  is the number of atoms in the system). Therefore, in the present study, we applied the direct ab initio dynamics method with all degrees of freedom. Details of the direct dynamics method are described elsewhere.<sup>11</sup>

First, a trajectory calculation of neutral system Bz–HF was carried out in order to obtain the initial structure of Bz<sup>+</sup>–HF after ionization. At the start of the trajectory calculation, atomic velocities are adjusted to give temperatures of both 10 and 50 K. Temperature is defined by

$$T = \frac{1}{3Nk} \left\langle \sum_{i=1}^N m_i v_i^2 \right\rangle$$

where  $N$  is number of atoms,  $v_i$  and  $m_i$  are velocity and mass of the  $i$ th atom, and  $k$  is Boltzmann's constant. Second, the geometrical configurations are chosen from the trajectory calculations for the neutral system. The velocities of atoms

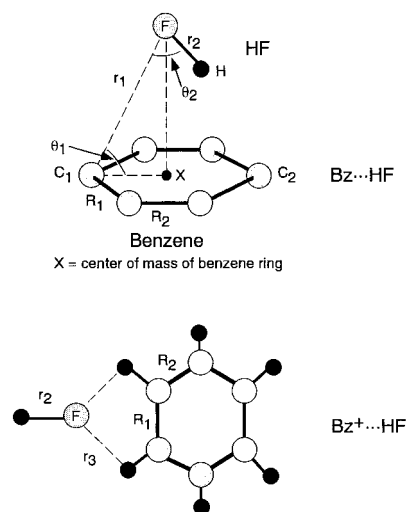


**Figure 1.** Structures and geometrical parameters of benzene–HF complex (Bz–HF) and its cation complex (Bz<sup>+</sup>⋯HF).

(i.e., momentum of each atom) were assumed to zero at the starting point on the cationic surface. We have selected twenty trajectories for each temperature.

The equations of motion for  $N$  atoms in a molecule are

$$\begin{aligned} \frac{dQ_j}{dt} &= \frac{\partial H}{\partial P_j} \\ \frac{\partial P_j}{\partial t} &= -\frac{\partial H}{\partial Q_j} = -\frac{\partial U}{\partial Q_j} \end{aligned}$$

where  $j = 1-3N$ ,  $H$  is the classical Hamiltonian,  $Q_j$  is Cartesian coordinate of the  $j$ th mode, and  $P_j$  is conjugate momentum. These equations were numerically solved by the Runge–Kutta method. No symmetry restriction was applied to the calculation of the gradients in the Runge–Kutta method. The time step size was chosen as 0.10 fs, and a total of 10000 steps were calculated for each trajectory. The drift of the total energy was confirmed to be less than 0.1% for an entire trajectory. It was also confirmed that the momentum of the center of mass and the angular momentum around the center of mass retained their initial values of zero.

In direct ab initio dynamics calculation, it generally requires a large CPU time and a large memory to generate even one trajectory. Because of this limitation, we used 3-21G\* basis set for the system the dynamics calculations. This level of theory may be limited in a general computer facility. A CPU time was about 2 days for one trajectory on a workstation (IBM-RS6000/RP43).

To obtain structures and energetics of the Bz–HF and Bz<sup>+</sup>–HF complexes in more details, ab initio MO calculations<sup>13</sup> were carried out at the HF and MP2 levels of theory with 3-21G\* and 6-31G\* basis sets.

## 3. Results

**I. Ab initio Molecular Orbital (MO) Calculations. A. Structure of the Neutral Complex Bz–HF.** The structures of the neutral complex Bz–HF are fully optimized at the HF/3-21G\*, HF/6-31G\*, and MP2/6-31G\* levels of theory. We assumed both  $C_s$  and  $C_{6v}$  symmetries in the optimization of the Bz–HF complex. The geometrical parameters used in the optimization are illustrated in Figure 1, while the optimized parameters are summarized in Table 1. All calculations gave the similar results: the H-end of HF points toward Bz as shown

**TABLE 1: Optimized Parameters for Bz–HF and Bz<sup>+</sup>–HF Complexes Calculated at the C<sub>s</sub> Symmetry<sup>a</sup>**

	HF/3-21G*	HF/6-31G*	MP2/6-31G*
Bz···HF			
R <sub>1</sub>	1.3874 (1.3861)	1.3884 (1.3875)	1.3991 (1.3983)
R <sub>2</sub>	1.3854	1.3872	1.3980
r <sub>1</sub>	3.2886 (3.3524)	3.4308 (3.6097)	3.3078 (3.3749)
r <sub>2</sub>	0.9393 (0.9384)	0.9135 (0.9129)	0.9367 (0.9361)
θ <sub>1</sub>	83.32	76.32	70.00
θ <sub>2</sub>	14.04	14.35	12.86
Bz <sup>+</sup> ···HF			
R <sub>1</sub>	1.4467	1.4444	1.4525
R <sub>2</sub>	1.3826	1.3848	1.3885
r <sub>1</sub>	2.8447	3.0848	4.3325
r <sub>2</sub>	0.9407	0.9157	0.9392
r <sub>3</sub>	2.1659	2.3874	2.2890

<sup>a</sup> The parameters obtained for C<sub>6v</sub> structures of Bz···HF are given in parenthesis. Bond lengths and angles are in angstrom and in degrees, respectively.

in Figure 1(upper). The bonding nature is composed of dipole–π-orbital interaction. The calculations show that the intermolecular distances between HF and Bz (defined by r<sub>1</sub>) are calculated to be 3.3078 Å (C<sub>s</sub>) and 3.3749 Å (C<sub>6v</sub>) at the MP2/6-31G\* level. The energy differences between C<sub>s</sub> and C<sub>6v</sub> structures are calculated to be 0.14 (HF/3-21G\*), 0.03 (HF/6-31G\*), and 0.02 kcal/mol (MP2/6-31G\*), suggesting that the HF molecule can move easily on Bz at finite temperature. Also, this result indicates that the Bz–HF complex has a nonrigid structure and a wide-Franck Condon (FC) region for the ionization.

**B. Structure of the Complex Cation Bz<sup>+</sup>···HF.** Structure of the ionized complex Bz<sup>+</sup>–HF is optimized at the same levels of theory. No symmetry restriction was employed in the calculations. The structure of Bz<sup>+</sup>–HF is quite different from that of Bz–HF. Figure 1 (lower) represents an illustration of the most stable structure of Bz<sup>+</sup>–HF. In this complex, the F-end of HF points toward Bz<sup>+</sup>, and the F atom is bound equivalently to two protons of Bz<sup>+</sup>. The complex has a C<sub>s</sub> symmetry in which all atoms are located on the molecular plane (xz-plane).

The complex is more stable in energy than its dissociation limit (Bz<sup>+</sup> + HF). The stabilization in Bz<sup>+</sup>–HF is due to a strong Coulomb attractive interaction between HF and Bz<sup>+</sup>. The ab initio calculations show that the cation complex Bz<sup>+</sup>–HF is bound by 0.66 eV (MP2/6-31G\*) and 0.63 eV (HF/3-21G\*) relative to its dissociation limit. This result indicates that the complex formation may occur after the photodissociation of Bz–HF. Also, it can be expected that the dynamics calculation at the HF/3-21G\* level would give a reasonable qualitative feature on the reaction dynamics.

**C. Potential Energy Surface of Bz<sup>+</sup>···HF Complex.** The potential energy surfaces (PESs) for the Bz<sup>+</sup>–HF complex are calculated as functions of two large amplitude motions (r<sub>1</sub> and θ<sub>2</sub>). Figures 2A and B show PESs calculated at the HF/6-31G\* and HF/3-21G\* levels of theory, respectively. The geometrical parameters except for the two motions (r<sub>1</sub> and θ<sub>2</sub>) are fixed to those of the neutral Bz–HF complex. The hatched region in Figure 2A indicates schematically the Franck–Condon (FC) region which is estimated roughly from the neutral PES. A dot on Figure 2A (point a) indicates the equilibrium point for the neutral Bz–HF complex. The open circle on the PES (point b) represents an arbitrary point with a large angle (θ<sub>2</sub>) on the PES. At point a, the direction of steepest descent of PES points toward the r<sub>1</sub> direction, whereas the corresponding direction at point b is θ<sub>2</sub>. Therefore, it is predicted that the trajectories from points a and b, which are illustrated by solid and broken arrows,

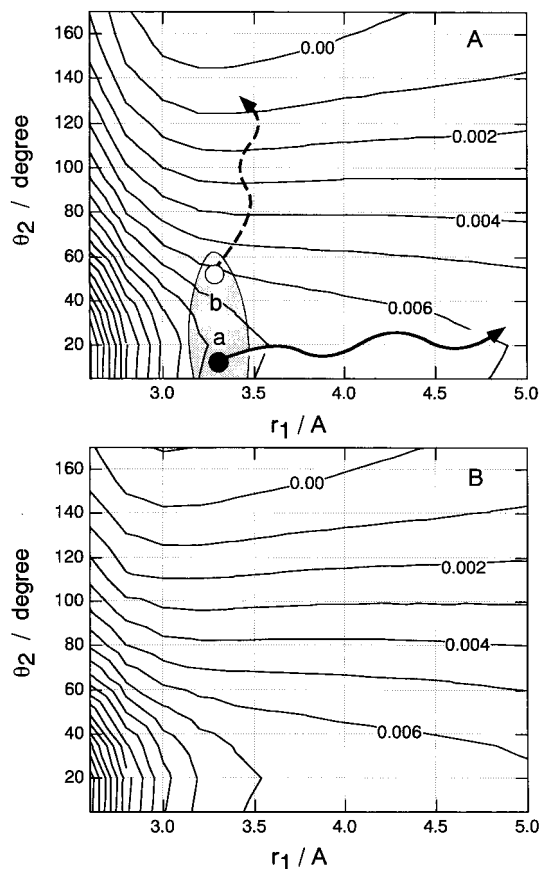


**Figure 2.** Potential energy surfaces for Bz<sup>+</sup>···HF complex calculated at the HF/6-31G\*(A) and HF/3-21G\* (B) levels as functions of r<sub>2</sub> and θ<sub>2</sub>. The other geometrical parameters are fixed to these of the optimized structure for Bz–HF complex. Contours are drawn in each 0.002 au. The open circle (point a) represents the equilibrium point of Bz–HF complex, while the closed circle represents an arbitrary point with a large θ<sub>2</sub> angle. Arrows indicate two typical trajectories for dissociation (solid line) and complex formation (broken line).

respectively, lead to the dissociation product (Bz<sup>+</sup> + HF) and complex formation one (Bz<sup>+</sup>···FH), respectively. This result implies that a trajectory ionized around the equilibrium point of Bz–HF leads to the dissociation channel (Bz<sup>+</sup> + HF), whereas a trajectory started from a large angle θ<sub>2</sub> leads to the complex formation channel. This feature will be confirmed by the following trajectory calculations in the next section.

The PES is also calculated by HF/3-21G\* calculation. The contour plot of PES is illustrated in Figure 2B. As clearly seen in this figure, the result obtained by the HF/3-21G\* calculation is essentially similar to that of HF/6-31G\*. This means that the dynamics calculation at the HF/3-21G\* level would give a reasonable result. At least, one can discuss the qualitative feature on the reaction dynamics using HF/3-21G\* calculation. It should be emphasized again that the purpose of this study is not to calculate accurate values of the product quantum states but to elucidate a qualitative feature of the ionization dynamics of the Bz–HF complex. Therefore, we use HF/3-21G\* method in the dynamics calculations throughout.

**II. Direct ab Initio Dynamics Calculations. A. Structure of the Neutral Complex.** First, trajectories are calculated for the neutral complex Bz–HF at both 10 and 50 K in order to obtain its structures at finite temperature. We have chosen 0.01 ps as a bath relaxation time, and the calculations were run from the optimized structure of the Bz–HF complex. Figure 3 shows the result of the trajectory calculation at 10 K. The potential energy of the system was close to a constant value (figure is

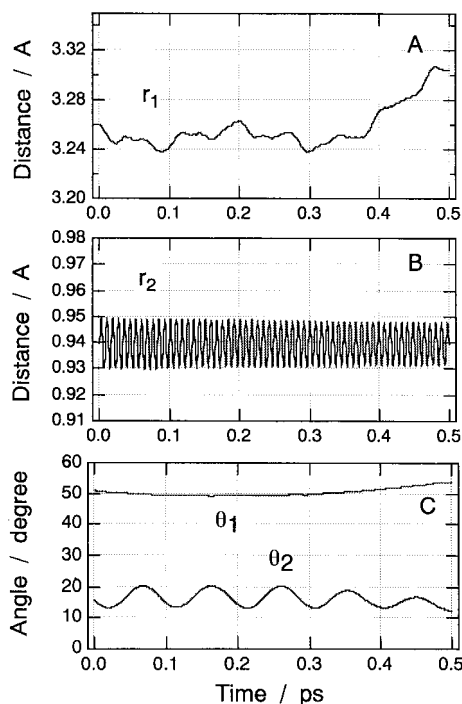


**Figure 3.** A trajectory for the neutral  $Bz\cdots HF$  complex plotted as a function of time. The simulation is carried out at 10 K. (A) Intermolecular distance  $r_1$ , (B) bond length of H–F ( $r_2$ ), and (C) angles ( $\theta_1$  and  $\theta_2$ ) versus time.

not given). The intermolecular distance between F and  $C_1$  atoms (denoted by  $r_1$ ) is plotted in Figure 3A as a function of simulation time. The distance ( $r_1$ ) oscillates slightly in the range 3.239–3.302 Å at 10 K. Time dependence of the H–F bond ( $r_2$ ) given in Figure 3B indicates that the H–F bond is periodically vibrated. Also, the angle of  $C_1$ –F– $H_0$  ( $= \theta_2$ ) fluctuated in the range 12–21°.

The similar simulation was carried out at 50 K. The intermolecular distance ( $r_1$ ) vibrates in the range 3.36–3.71 Å at 50 K, which is wider than that of 10 K. Also, the angle of  $C_1$ –F– $H_0$  ( $\theta_2$ ) fluctuated significantly in the range 10°–70°. From these results, it is expected that the  $Bz$ –HF complex has a nonrigid structure and a wide Franck–Condon (FC) region for the ionization even at lower temperatures (10–50 K).

**B. Ionization Processes of the  $Bz$ –HF Complex.** As suggested in Section IIA, the ionization occurs from the wide FC region. Hence we have chosen several points on the FC region as initial geometrical configurations in the dynamics calculations of  $Bz^+$ –HF. For each temperature (10 or 50 K), 12 trajectories were run from the initial structures which are selected randomly from the result for the neutral complex  $Bz$ –HF (given in section IIA). We assumed zero velocity of each atom at time zero on the cationic PES. The trajectory calculations of  $Bz^+$ –HF at 10 K show that all trajectory calculations gave the similar results: the trajectory leads only to the dissociation channel ( $Bz^+ + HF$ ). On the other hand, the dynamics calculations from the geometrical configurations at 50 K gave two reaction channels: the dissociation and complex formation channels. In this section, we will discuss the two reaction channels using the typical sample trajectories at 50 K.

**III. Dissociation Channel.** A sample trajectory for the dissociation channel (i.e., the products are  $Bz^+ + HF$ ) is given in Figure 4. Figure 4A shows the potential energy of the system (PE) calculated as a function of reaction time, while the intermolecular ( $r_1$ ), interatomic ( $r_2$ ) distances, and bond angles ( $\theta_1$  and  $\theta_2$ ) are plotted as a function time in Figure 4D,

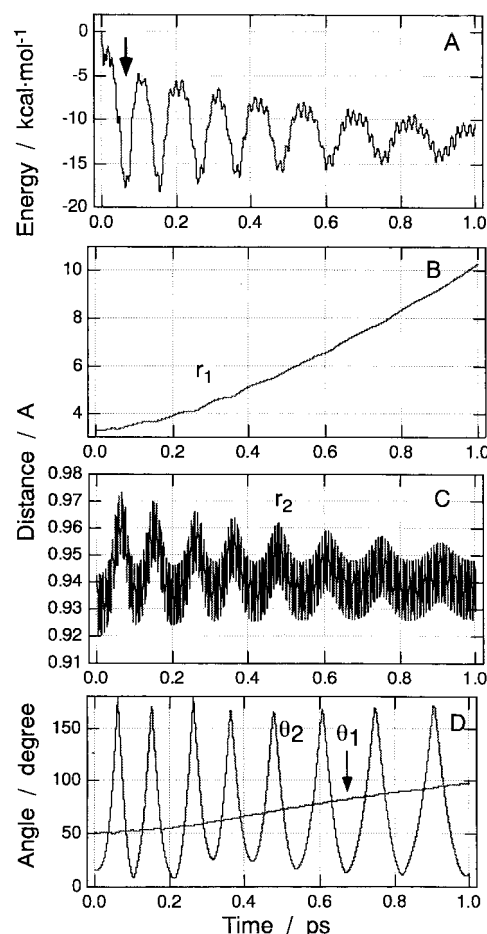


**Figure 4.** A sample trajectory for dissociation channel following the ionization of  $Bz$ –HF complex. (A) the potential energy of the reaction system, (B) intermolecular distance  $r_1$ , (C) bond length of H–F ( $r_2$ ), and (D) angles ( $\theta_1$  and  $\theta_2$ ) versus time. Allows indicate one of the valley of potential energy formed by the dipole interaction between HF and  $Bz^+$ .

respectively. Zero level of PE corresponds to the energy at the starting point on PES of  $Bz^+$ –HF. Within a very short time region (0–0.02 ps), PE decreases suddenly to  $-3.0$  kcal/mol because of the Jahn–Teller effect produced by the benzene ring.<sup>14</sup> After that, the PE decreases more deeply (as indicated by arrow in Figure 4A) and oscillates periodically as a function of reaction time. As seen in the PE curve, both valley and peak appear each  $\sim 0.05$  ps (the valley is indicated by the arrow). To elucidate these features, the angle  $\theta_2$  (which is close to the angle between dipole of HF and the benzene  $C_6$  axis) is analyzed in details. By comparing PE and  $\theta_2$  (Figures 4A and D), it is found that the time period of the valley peak corresponds completely to the rotation period of the HF molecule. That is, the minimum of PE appears when the dipole of HF points toward  $Bz^+$  (i.e., the F end of HF molecule points toward  $Bz^+$ ). On the other hand, the peak appears when the H-end of HF points toward  $Bz^+$ . These results imply that the dipole–charge interaction between HF and  $Bz^+$  dominates strongly the dynamics after ionization. After longer simulation time ( $> 0.6$  ps), the energy minimum of the valley becomes shallower, suggesting that the interaction becomes weaker at longer separation of HF and  $Bz^+$ .

Figure 4B shows that the intermolecular distance between F and  $C_1$  atoms ( $r_1$ ) increases monotonically as a function of reaction time. This means that the HF molecule is dissociated directly from  $Bz^+$ . Also, the time-dependence of the  $H_0$ –F– $C_1$  angle ( $\theta_2$ ) plotted in Figure 4D shows that the angle is strongly varied in the range 0–180° as a function of reaction



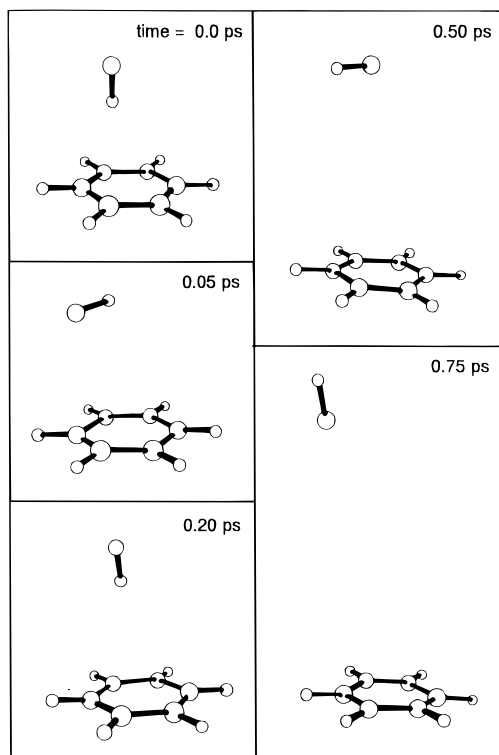


**Figure 5.** Snapshots for dissociation channel following the ionization of  $Bz^+\cdots HF$  complex. The energy and geometrical parameters versus time are given in Figure 4.

time. This is due to the fact that the rotational mode of HF is excited. These results indicate that the HF molecule is dissociated by accompanying with the rotational excitation after the ionization of  $Bz-HF$ .

The time-dependence of H-F bond distance is plotted in Figure 4C. It is seen that the equilibrium nuclear distance of HF is periodically switched between 0.93 and 0.96 Å at the first stage of the dissociation (0–0.2 ps). The time period corresponds completely to that of  $C_1-F-H_0$  ( $\theta_2$ ) angle, suggesting that the equilibrium nuclear distance of HF is elongated when the dipole of HF points toward  $Bz^+$  (0.96 Å). On the other hand, the distance is shortened when the H-end of HF points toward  $Bz^+$ . This result indicates that the interaction between HF and  $Bz^+$  is strong at the first stage of the ionization. At longer separation, the equilibrium nuclear distance of HF is converged to the normal H-F distance.

Relative translational energy between  $Bz^+$  and HF is estimated by 1.2 kcal/mol<sup>-1</sup> which corresponds to 10% of total available energy. The rotational quantum number of HF molecule is estimated by  $J = 1$ . These results indicate that almost available energy is partitioned into the internal modes of  $Bz^+$ .

Snapshots of the geometrical configurations of  $Bz^+-HF$  are illustrated in Figure 5. At time zero, the complex has the structure where the H-end of HF points toward  $Bz^+$ . After the ionization (at 0.05 ps), the HF molecule is rotated by a strong repulsive interaction between the proton and  $Bz^+$ . After that, the HF molecule leaves away from  $Bz^+$  with the rotation. After 0.75 ps, the HF molecule is fully separated from  $Bz^+$ , and the interaction between HF and  $Bz^+$  becomes negligibly small. Therefore, this trajectory leads to the dissociation channel.

**IV. Complex Formation Channel.** A sample trajectory for the complex formation channel (the product is the cation complex  $Bz^+\cdots FH$ ) is given in Figure 6. It should be noted that the angle  $\theta_2$  at time zero is 52° which is much larger than

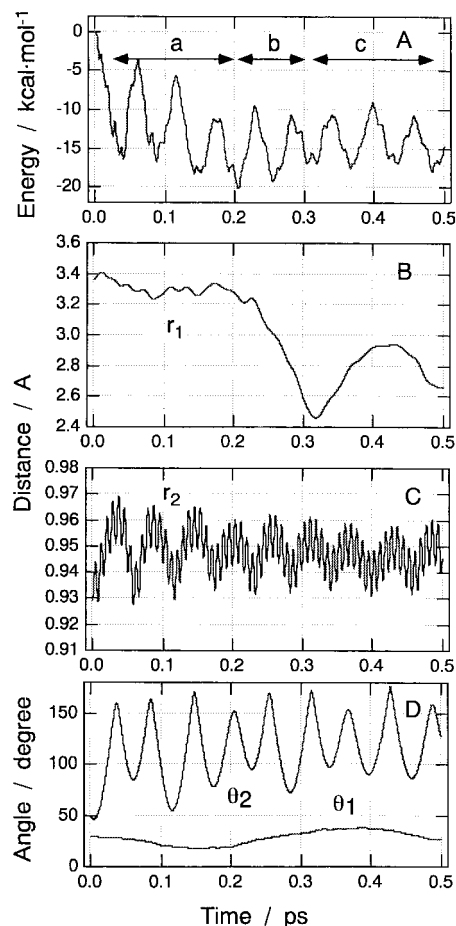


**Figure 6.** A sample trajectory for complex formation channel following the ionization of  $Bz^+\cdots HF$  complex. (A) the potential energy of the reaction system, (B) intermolecular distance  $r_1$ , (C) bond length of H-F ( $r_2$ ), and (D) angles ( $\theta_1$  and  $\theta_2$ ) versus time. Allows in Figure 6A indicate three stages of the reaction (See text).

that of the dissociation channel (given in Figures 4 and 5). The reaction for the complex formation channel is composed of three stages which are expressed by “HF rotation”, “HF approaching”, and “complex formation”. These stages are defined approximately by regions **a**, **b**, and **c**, respectively, as shown in Figure 6A. At time zero, the interaction between  $Bz$  and HF is changed suddenly from attractive to repulsive by the ionization. The repulsive interaction is caused by the Coulomb interaction between the proton of HF and  $Bz^+$ . The hydrogen-orientation form (i.e., the H-end of HF orients toward  $Bz^+$ ) is higher in energy than that of the dissociation limit ( $Bz^+ + HF$ ). On the other hand, the configuration whose the F end of HF points toward  $Bz^+$  is stable than that of the dissociation limit. The HF is rotated in order to prevent the repulsion at the first stage (region **a**, 0–0.20 ps). After that, HF approaches slightly  $Bz^+$ . At 0.20 ps, the attractive force between HF and  $Bz^+$  becomes larger than the repulsive force, so that HF approaches rapidly  $Bz^+$ . This approaching process of HF corresponds to the second stage which is denoted by region **b**. At 0.32 ps, the intermolecular distance  $r_1$  is minimized enough to form the cation complex. In the third stage, which is denoted by region **c** (0.32–0.50 ps), the rotation of HF is quenched by forming the  $Bz^+-HF$  complex. The reaction is completed at the third stages.

Snapshots of the geometrical configurations for the complex formation channel are given in Figure 7. Note that the dipole of HF at time zero does not point toward  $Bz^+$  as shown in Figure 7. At time zero, the angle ( $\theta_2$ ) takes about 52° in this sample trajectory. By the ionization of the  $Bz-HF$  complex, the rotation

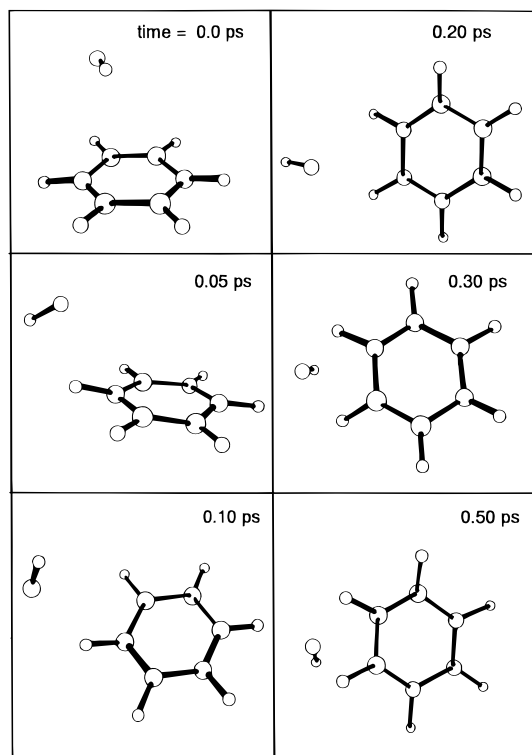


**Figure 7.** Snapshots for complex formation channel following the ionization of Bz–HF complex. The energy and geometrical parameters versus time are given in Figure 6.

**TABLE 2: Summary of Trajectory Calculations for Bz<sup>+</sup>–HF System Started from Randomly Selected Points on the Franck-Condon Region<sup>a</sup>**

$\theta_2/\text{degree}$	$r_1/\text{\AA}$	product channel	comment
12.52	3.2132	dissociation	
13.51	3.2386	dissociation	
14.04	3.2886	dissociation	equilibrium point
19.05	3.1752	dissociation	
21.40	3.2129	dissociation	
22.24	3.1432	dissociation	
23.70	3.5268	dissociation	
27.80	3.1635	complex	
28.01	3.1707	complex	
33.22	3.0900	complex	
52.29	2.9010	complex	
68.52	3.1421	complex	

<sup>a</sup> The simulation of neutral complex Bz<sup>+</sup>••HF was carried out at 50 K.

of HF is excited due to the repulsive interaction between Bz<sup>+</sup> and HF proton. After 0.05–0.10 ps, the HF molecule moves rapidly to near the molecular plane of Bz<sup>+</sup>. At 0.20 ps, the F atom of HF points toward Bz<sup>+</sup>, and the hydrogen bond between F and protons of Bz<sup>+</sup> is formed. The structural configuration at 0.20 ps is significantly close to the complex cation of Bz<sup>+</sup>–FH as suggested in section I. Finally, the trajectory leads to the complex formation. In the case of the sample trajectory, the complex formation process is almost completed at 0.2–0.3 ps.

**V. Summary of Dynamics Calculations.** The results of the dynamics calculations at 50 K are summarized in Table 2. Twelve trajectories, selected randomly from the geometrical configurations at 50 K, were calculated. It was found that two reaction channels are concerned with the ionization of the Bz–HF complex. These are direct dissociation and complex formation channels. As clearly seen in Table 2, the ionization of the Bz–HF complex with smaller angle ( $\theta_2$ ) leads to dissociation channel, whereas the ionization from larger angles leads to the

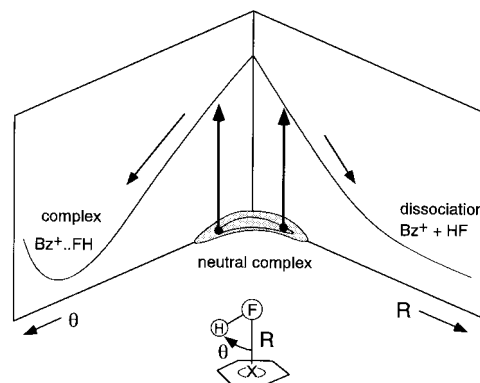


**Figure 8.** Reaction model for the photoionization processes of Bz–HF. Right and left parts show the potential energy curves for dissociation and complex formation channels following the vertical ionization of Bz–HF complex, respectively.

complex formation channel. Also, it is found that the reaction channel is insensitive to the initial separation between HF and Bz (i.e., the distance  $r_1$ ). Both channels compete against each other at 50 K. On the other hand, at 10 K the direct dissociation is only observed as a product channel. Thus, the present study predicts that the product channels are strongly dependent on temperature of neutral complex Bz–HF before the ionization.

#### 4. Discussion

**Model of the Photoionization Dynamics of Bz–HF.** In this study, we investigated the ionization processes of the Bz–HF complex by means of direct ab initio dynamics method. On the basis of the present results, we propose a reaction model for the ionization processes of Bz–HF. Potential energy curves (PECs) for the ionization processes of Bz–HF are schematically illustrated in Figure 8. The reaction coordinates after the ionization are expressed approximately by two large amplitude motions ( $R$  and  $\theta$ ), where  $R$  is a distance between the center-of-mass of Bz<sup>+</sup> and the F atom and  $\theta$  is angle H–F–X (denoted by X) and the hatched region represents schematically the FC region for the ionization. If the ionization occurs at small angle  $\theta$ , the dissociation channel (Bz<sup>+</sup> + HF) is dominant. On the other hand, the ionization from a large angle leads to the complex formation channel. This preference is originated from the Coulomb repulsive interaction between proton of HF and ionized Bz<sup>+</sup>. In the case of small angle  $\theta$ , the interaction between the proton and Bz<sup>+</sup> is strongly repulsive. The HF molecule leaves rapidly from Bz<sup>+</sup> before the complex formation. If the ionization occurs from larger angle  $\theta$ , the repulsion becomes smaller, so that the complex can form without the direct dissociation.

On the basis of the theoretical results, it can be predicted that two product channels are competitive on the photoionization of Bz–HF. The photoionization from the small angle  $\theta$  on FC region (i.e., the ionization at low temperature) leads to the dissociation channel due to the fact that the potential energy surface is strongly repulsive. The HF molecule dissociates rapidly from benzene ring (Bz<sup>+</sup>). This dissociation will be completed within 0.5 ps. On the other hand, on the photoionization from the larger angles on FC region (i.e., the ionization at higher temperatures), a long-lived complex channel is open in addition to the direct dissociation channel. The lifetime of the complex Bz<sup>+</sup>••FH is at least longer than 2.0 ps.

Here let us consider ideal experiment to confirm the present model. From the present study, it can be expected that the ionization of BzHF at low-temperature leads to the dissociation products (Bz<sup>+</sup> + HF), whereas the ionization at higher tem-

peratures (over 50 K) leads to the complex formation. These results mean that the  $\text{BzHF}^+$  cation would be detected by mass spectrometry, if  $\text{BzHF}$  is photoionized at higher temperatures. On the other hand,  $\text{Bz}^+$  is only detected in the case of the ionization at low temperature. In recent developed experiments, it is possible to control the temperature of cluster in supersonic jet. Therefore, our model will be confirmed by experiment in the near future.

### 5. Concluding Remarks

We have introduced several approximations to calculate the potential energy surface and to treat the reaction dynamics. First, we assumed that the  $\text{Bz}^+\text{--HF}$  complex have no excess energy at the initial step of the trajectory calculation (time = 0.0 ps). This may cause slight change of lifetime and energy distribution of the  $\text{Bz}^+\text{--HF}$  complex. In the case of higher excess energy, the dissociation of HF may occur more efficiently in the  $\text{Bz}^+\text{--HF}$  complex. This effect was not considered in the present calculations. It should be noted therefore that the present model is limited in the case of no excess energy.

Second, we assumed HF/3-21G\* multidimensional potential energy surface in the trajectory calculations throughout. As shown in section I, the shape of PES for the  $\text{Bz}^+\text{--HF}$  system calculated by HF/3-21G\* is in good agreement with that of HF/6-31G\*. However, in the neutral  $\text{Bz}\text{--HF}$  complex, the HF/3-21G\* calculation give a shorter intermolecular distance ( $r_1$ ) due to the basis set super position error (BSSE). To check the effect of the ionization point (for the  $r_1$  direction) on the dynamics, the direct dynamics calculations from three ionization points (we have chosen  $r_1 = 3.00, 3.25, \text{ and } 3.50 \text{ \AA}$ ) were examined. All calculations gave the similar results. This is due to the fact that the product channel is mainly dominant by the angle  $\theta$ . Hence the HF/3-21G\* level of theory would be adequate to discuss *qualitatively* the photoionization dynamics of  $\text{Bz}\text{--HF}$  as shown in the present paper, although more accurate wave function may provide deeper insight in the dynamics (for example, the branching ratio of the product channels). Despite the several assumptions introduced here, the results enable us

to obtain valuable information on the mechanism of the photoionization processes in  $\text{Bz}\text{--HF}$  complex.

**Acknowledgment.** The author is indebted to the Computer Center at the Institute for Molecular Science (IMS) for the use of the computing facilities. The author acknowledges partial support from a Grant-in-Aid from the Ministry of Education, Science, Sports and Culture of Japan.

### References and Notes

- (1) Müller-Dethlefs, K.; Dopfer, O.; Wright, T. G. *Chem. Rev.* **1994**, *94*, 1845.
- (2) Gonohe, N.; Abe, H.; Mikami, N.; Ito, M. *J. Phys. Chem.* **1985**, *89*, 3462.
- (3) (a) Zwier, T. S. *Annu. Rev. Phys. Chem.* **1996**, *47*, 205 and references therein. (b) Gotch, A. J.; Zwier, T. S. *J. Chem. Phys.* **1992**, *96*, 3388.
- (4) Hutson, J. M. *J. Chem. Phys.* **1992**, *96*, 6752.
- (5) Hutson, J. M. *J. Phys. Chem.* **1992**, *96*, 4237.
- (6) Cohen, R. C.; Saykally, R. J. *J. Chem. Phys.* **1993**, *98*, 6007.
- (7) Schmuttermmaer, C. A.; Cohen, R. C.; Saykally, R. J. *J. Chem. Phys.* **1994**, *102*, 146.
- (8) Courty, A.; Mons, M.; Calve, J. Le; Piuze, F.; Dimicoli, I. *J. Phys. Chem. A* **1997**, *101*, 1145.
- (9) Balocchl, F. A.; Williams, J. H.; Klemperer, W. *J. Phys. Chem.* **1983**, *87*, 2079.
- (10) Cheney, B. V.; Schulz, M. W.; Cheney, J.; Richards, W. G. *J. Am. Chem. Soc.* **1988**, *110*, 4195.
- (11) (a) Tachikawa, H.; Igarashi, M. *J. Phys. Chem. A* **1998**, *102*, 8648. (b) Tachikawa, H. *J. Phys. Chem. A* **1997**, *101*, 7475. (c) Tachikawa, H. *J. Phys. Chem. A* **1998**, *102*, 7065. (d) Tachikawa, H. *J. Phys. Chem.* **1996**, *100*, 17090. (e) Program code of the direct ab initio dynamics calculation was created by our group.
- (12) (a) Tachikawa, H. *J. Chem. Phys.* **1998**, *108*, 3966. (b) Tachikawa, H. *J. Phys. Chem.* **1995**, *99*, 225. (c) For a review article, see: Tachikawa, H. *Trend Phys. Chem.* **1997**, *6*, 279.
- (13) Ab initio MO calculation program: Frisch, M. J.; Trucks, G. W.; Schlegel, H. B.; Gill, P. M. W.; Johnson, B. G.; Robb, M. A.; Cheeseman, J. R.; Keith, T.; Petersson, G. A.; Montgomery, J. A.; Raghavachari, K.; Al-Laham, M. A.; Zakrzewski, V. G.; Ortiz, J. V.; Foresman, J. B.; Cioslowski, J.; Stefanov, B. B.; Nanayakkara, A.; Challacombe, M.; Peng, C. Y.; Ayala, P. Y.; Chen, W.; Wong, M. W.; Andres, J. L.; Replogle, E. S.; Gomperts, R.; Martin, R. L.; Fox, D. J.; Binkley, J. S.; Defrees, D. J.; Baker, J.; Stewart, J. P.; Head-Gordon, M.; Gonzalez, C.; Pople, J. A.: *Gaussian 94*, Revision D.3; Gaussian, Inc.: Pittsburgh, PA, 1995.
- (14) Iwasaki, M.; Toriyama, K.; Nunome, K., *J. Chem. Soc. Chem. Commun.* **1983**, 320.